Correlating atomic structure and transport in suspended graphene nanoribbons

-- Supporting Information --

Zhengqing John Qi[1†], Julio A. Rodríguez-Manzo[1†], Andrés R. Botello-Méndez[2], Sung Ju Hong[1,3], Eric A. Stach[4], Yung Woo Park[3], Jean-Christophe Charlier[2], Marija Drndić[1*], and A. T. Charlie Johnson[1**]

[1]*Department of Physics and Astronomy, University of Pennsylvania, Philadelphia, Pennsylvania 19104, USA.*

[2]*Institute of Condensed Matter and Nanosciences, Université catholique de Louvain, Chemin des étoiles 8, 1348 Louvain-la-Neuve, Belgium.*

[3]*Department of Physics and Astronomy, Seoul National University, 1 Gwanak-ro, Gwanak-gu, Seoul, 151-747, Korea.*

[4]*Center for Functional Nanomaterials, Brookhaven National Laboratory, Upton, New York 11973, USA.*

† These authors contributed equally to this work.

* Correspondence to Marija Drndić, drndic@physics.upenn.edu

** Correspondence to A. T. Charlie Johnson, cjohnson@physics.upenn.edu

Details of device fabrication

Devices were based on Si/SiN substrates obtained from WRS Materials with a 100 nm-thick low stress (<100 MPa) SiN layer that was deposited by low pressure chemical vapor deposition (CVD). Nitride membranes of dimensions 40 × 40 μm^2 were micromachined using standard silicon wet etching in KOH. Electron beam lithography was used to pattern source-drain electrodes that extend onto the membrane, which were then metallized with thermally evaporated chromium/gold (10 nm/100 nm). A 150-nm-wide slit was defined between the contacts by focused ion beam milling using a 10 pA Ga ion beam (FEI Strata DB235). Large-area graphene grown by atmospheric pressure CVD[1] was transferred onto the Si/SiN chip and patterned into a ribbon that crossed over the slit using electron beam lithography (negative-tone resist XR-1541, Dow Corning) followed by O_2 plasma etching (Technics PE II-A, 50 W for 20 s). Control of graphene growth parameters allowed for the fabrication of both few- and mono-layer graphene ribbons.

Methods for quantum transport calcualtions

Quantum transport calculations were performed within a tight-binding model and the Landauer formalism. The tight-binding model consists of a single p-orbital per carbon atom and a third nearest neighbor interaction. The hopping integrals and the on-site energies at the borders were parameterized to reproduce the gap of the three armchair families calculated by means of GW calculations[2]. The out of plane interaction was modeled after Slonczewski-Weiss-McClure[3]. The Landauer conductance was computed using the tight binding Hamiltonian, and the Green's function surface matching method [4].

Calcualtions for sputtering rate of C atoms from the electron beam

The displacement rate per atom is defined as $p = \sigma \times j$, where σ is the cross section for atom displacements and j the electron beam current density. Considering a current density of $j \sim 10$ A/cm^2, as in our experiment, and $\sigma = 2.8 \times 10^{-27}$ m^2 (for a 15 eV threshold displacement energy[5]), the value for $p \sim 0.002$ displacements per C atoms in one second. For GNRs under high bias the displacement rate should be less than this, considering that the high temperature of the system allows filling of vacancies from nearby diffusing C atoms. Therefore, in 1 minute each atom of C should be displaced less than 0.1 times during observation. A single layer of graphene under

these conditions (300 keV) would require more than 10 minutes of electron irradiation to fully collapse. In our experiments, the time to breakdown was much shorter, of order 1 min. GNR breakage thus is not due only to electron beam damage; other effects such as the high voltage bias and mechanical stress must be considered. For GNR cutting, the current density was increased two or three orders of magnitude.

Supplementary Video 1

Bonded bilayer GNR at its minimum width (0.7 nm) before breakage. The movie was made by joining 61 CCD images, with one second exposure for each image. For clarity, the movie runs eight times faster (8 fps) than reality. To improve visibility the background of all the images were flattened and a Gaussian filter of 1 pixel radius was applied to filter out high frequency noise.

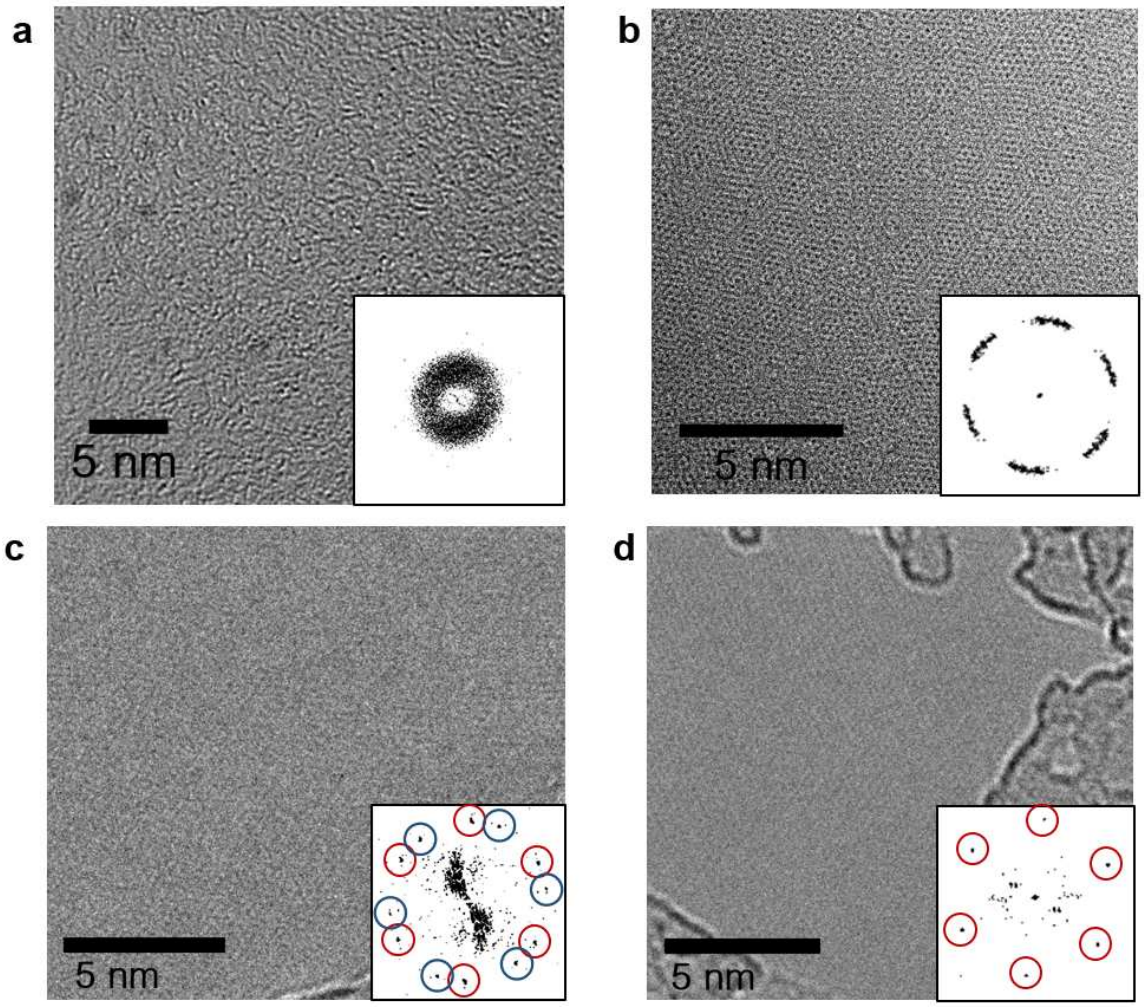

Figure S1. High-resolution TEM micrographs of (a) GNR device before annealing. The remaining panels are of devices after annealing, all with nearly pristine surfaces. (b) few-layer GNR; (c) bi-layer GNR; (d)) monolayer GNR. Insets are the corresponding 2D FFT, showing how the layer number can be inferred from the number of distinct 6-fold FFT peaks.

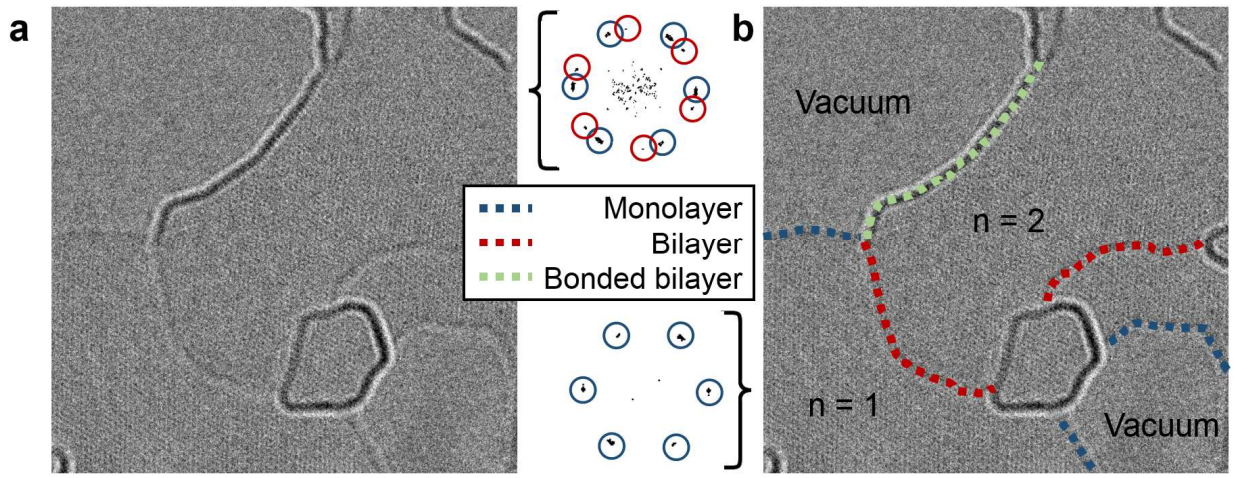

Figure S2. (a) TEM micrograph of a graphene island supported by a bulk monolayer sheet. Corresponding 2D FFT shows a single-layer region, labeled "n = 1" in (b), and a bilayer region, labeled "n = 2". Edge contrast allows for a clear distinction between monolayer, bilayer (unbound), and bonded bilayer edges. (b) Edges from panel (a) identified and highlighted. The blue dashed line marks a single-layer edge. The red dashed line represents the termination of a monolayer island that is being supported by the single-layer graphene substrate; an isolated bilayer graphene edge. The green dashed line represents a sp^2-bonded edge structure, illustrated by the darker edge contrast that originates from additional electron scattering at the bonded edge.

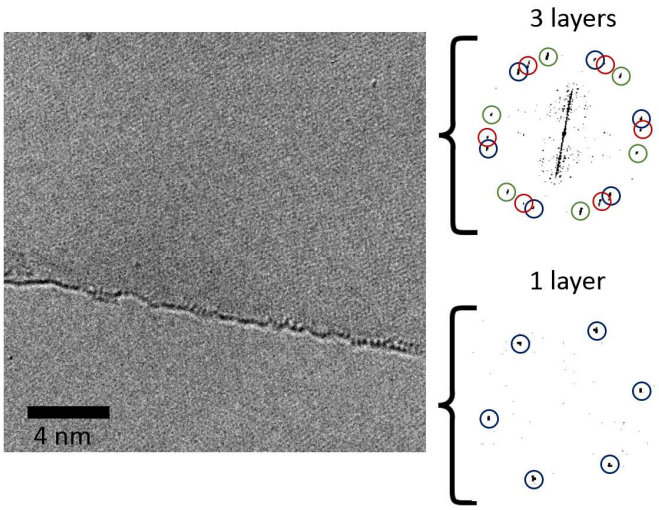

Figure S3. TEM micrograph of a three-layer graphene sheet (top) and a single-layer graphene sheet (bottom) separated by a single sp^2-bonded edge. Number of layers is extracted from the 2D FFT.

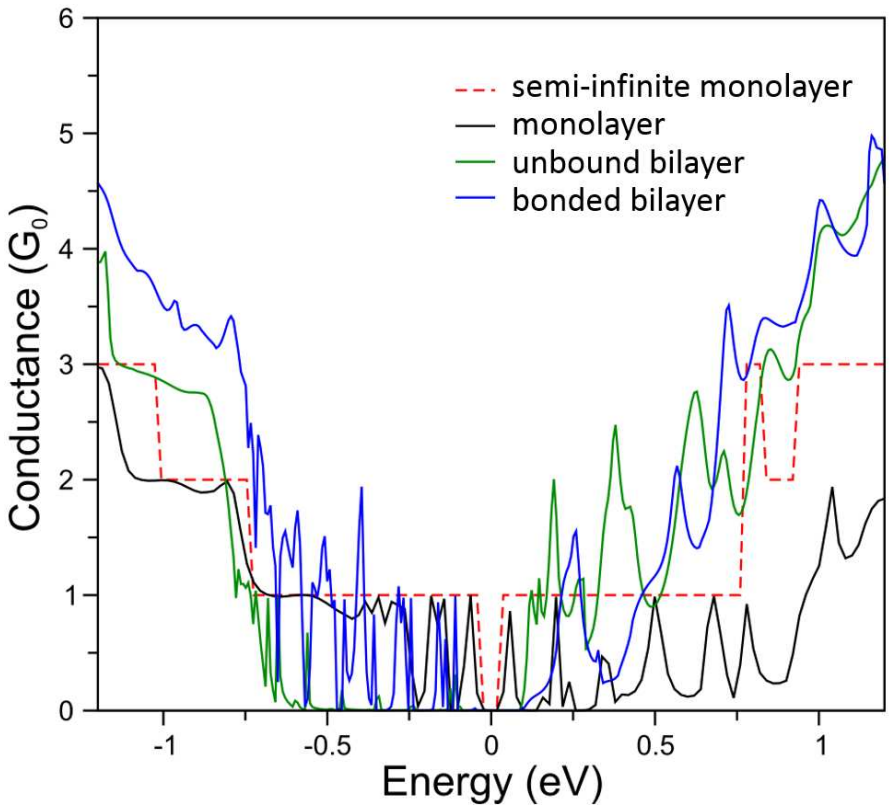

Figure S4. Quantum conductance characteristics of different GNR devices. The dashed red line is a plot of the quantum conductance of a pristine monolayer GNR ca. 2nm in width. When this GNR is used as a channel between two wider (ca. 30nm) GNR halves (see Fig. 5b), the conductance (black curve) exhibits oscillations close to the charge neutrality point due to constructive and destructive interferences, as in a Fabry-Perot interferometer. In a bilayer device with free (not bonded) edges (green curve), large scattering is observed for the holes, and the electrons exhibit a large increase in conductance due to additional channels (normally 2x). A bonded (or "looped") bilayer GNR exhibits less edge scattering and, since coherence along the channel is restored, interference oscillations re-appear.

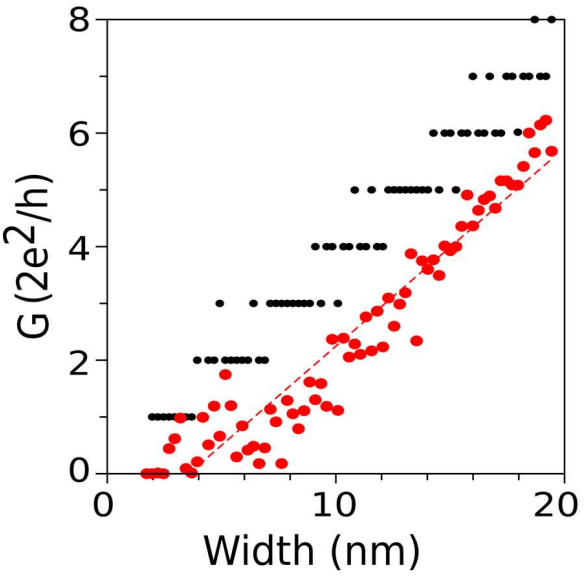

Figure S5. Simulation of the conductance as a function of width for an armchair monolayer GNR. Black points represent the ideal semi-infinite armchair terminated GNRs, while red points are the results including reflection and scattering due to contact effects.

1. Luo, Z.; Lu, Y.; Singer, D. W.; Berck, M. E.; Somers, L. A.; Goldsmith, B. R.; Johnson, A. T. C., Effect of Substrate Roughness and Feedstock Concentration on Growth of Wafer-Scale Graphene at Atmospheric Pressure. *Chem. Mater.* **2011,** *23*, 1441-1447.
2. Yang, L.; Park, C.-H.; Son, Y.-W.; Cohen, M. L.; Louie, S. G., Quasiparticle Energies and Band Gaps in Graphene Nanoribbons. *Phys. Rev. Lett.* **2007,** *99* (18), 186801.
3. Botello-Mendez, A. R.; Cruz-Silva, E.; Romo-Herrera, J. M.; López-Urias, F.; Terrones, M.; Sumpter, B. G.; Terrones, H.; Charlier, J.-C.; Meunier, V., Quantum transport in graphene nanonetworks. *Nano Lett.* **2011,** *11*, 3058-3064.
4. Meunier, V.; Sumpter, B. G., Amphoteric doping of carbon nanotubes by encapsulation of organic molecules: Electronic properties and quantum conductance. *J. Chem. Phys.* **2005,** *123*, 024705.
5. Banhart, F., Irradiation effects in carbon nanostructures. *Reports on progress in physics* **1999,** *62*, 1181.